Research on Chemical Intermediates (2019) 45:2065–2078
https://doi.org/10.1007/s11164-018-03717-9

Synthesis of zinc oxide nanoparticles (ZnO NPs) using pure bioflavonoid rutin and their biomedical applications: antibacterial, antioxidant and cytotoxic activities

Devaraj Bharathi[1] · **V. Bhuvaneshwari**[1]

Received: 19 October 2018 / Accepted: 14 December 2018 / Published online: 2 January 2019

Abstract

The present study reports an eco-friendly green synthesis of zinc oxide nanoparticles (ZnO NPs) using the bioflavonoid rutin. The synthesized ZnO NPs were characterized by UV–visible spectroscopy, XRD, FE-SEM, EDX, FTIR and zeta potential analyses. FE-SEM image showed that the synthesized ZnO NPs were rod shaped. FTIR spectral studies confirmed the role of bioflavonoid rutin for the reduction, capping and synthesis of ZnO NPs. The green synthesized ZnO NPs showed significant antibacterial activity against both Gram-positive (*B. subtilis* and *S. aureus*) and Gram-negative (*K. pneumoniae* and *E. coli*) bacterial pathogens. However, the synthesized ZnO NPs were more effective against Gram-negative bacteria compared to Gram-positive bacteria. The in vitro antioxidant ability of ZnO NPs was investigated spectrophotometrically using DPPH and H_2O_2 assay. The percentage of antioxidant activity increased with increasing concentration of ZnO NPs. Furthermore, synthesized ZnO NPs showed effectiveness in inhibiting the human MCF-7 breast cancer cells. In conclusion, the synthesized ZnO NPs using bioflavonoid rutin might be used as a strong biocidal and antioxidant agent in biomedical and pharmaceutical industries.

Keywords Rutin · Zinc oxide nanoparticles · Antibacterial agents · Antioxidant activity · Cytotoxic activity

Introduction

Nanobiotechnology is emerging as a fast developing research area with various applications in biomedical and pharmaceutical industries [1]. Recently, metal oxide nanoparticles of zinc, copper, iron, and cerium oxide have been the focus

✉ V. Bhuvaneshwari
bhuvanabt@yahoo.com; bhuvana_bt@yahoo.co.in

[1] Department of Biotechnology, Kongunadu Arts and Science College, Coimbatore, Tamilnadu 641 029, India

of interest due to their unique physical, chemical, and biological properties [2]. Among these metal oxide nanoparticles, zinc oxide nanoparticles (ZnO NPs) are often preferred due to their nontoxicity and are applied in various fields [3, 4].

Synthesis of ZnO NPs has been carried out by different methods such as precipitation [5], sol–gel [6], microwave assist [7], sonochemical synthesis [8], thermal decomposition [9], hydrothermal synthesis [10], and electrochemical [11]. All of these chemical and physical methods involve the use of toxic chemicals, which lead to harmful environmental problems [12]. Recently, a green chemistry method for the synthesis of ZnO NPs, especially using phyto-compounds, has gained significant importance because it is simple, low cost and environmentally friendly [13, 14].

Multiple human diseases caused by Gram-positive and Gram-negative bacteria are becoming resistant to commercial antibiotics, phyto-compounds and also natural traditional medicines [15]. The development of bacterial resistance to commercial antibiotics has become a major issue to bio-pharma industries and human health [16]. So there is an urgent need for the development of new biocidal agents against multi-drug resistant bacterial pathogens. In recent times, ZnO NPs show the impact of eradicating the bacterial pathogens with low cost and also an eco-friendly manner [17]. In a recent study, Ali et al. [18] reported that the synthesis of ZnO NPs from phytocompounds of *Conyza canadensis* showed significant antibacterial activity against bacterial pathogens. Moreover, ZnO NPs has various other biomedical applications such as antioxidant [17], antifungal [3], and cytotoxic activity against cancer cells [19].

The bioflavonoid rutin is a polyphenol compound found in many medicinal plants and vegetables [20]. It has potential bioactive properties such as strong antioxidant activity of the plant origin [21], cytotoxic and anti-proliferative activities [22]. It prevents the proliferation of human lung and colon carcinoma cells [23]. However, the bacterial pathogen killing ability of rutin and synthesis of metal oxide nanoparticles using this commercially and biologically valuable flavonoid has gained less attention. Hence, the present study aimed to synthesis ZnO NPs using pure bioflavonoid rutin compound for the first time. Here, we have demonstrated the synthesis, characterization and antibacterial activity of ZnO NPs. In addition, antioxidant properties of ZnO NPs by two methods (DPPH and H_2O_2), and cytotoxic activity against breast cancer cell line was discussed.

Experimental

Chemicals

Zinc sulphate, rutin, Meuller-Hinton agar (MHA), 2,2-diphenyl-1-picrylhydrazyl (DPPH), 3-[4,5-96 dimethylthiazole-2-yl]-2,5-diphenyltetrazolium bromide (MTT), Dulbecco's modified Eagle medium (DMEM) were obtained from Himedia Laboratories. All other chemicals and reagents used in this study were of analytical grade. The experiments in this study were done using sterile distilled water.

Synthesis of zinc oxide nanoparticles

About 20 mL of aqueous rutin (0.2 mM) was added into 20 mL of zinc sulphate (0.5 M) solution in a 100-mL conical flask, and the reaction mixture was subjected to continuous stirring with a magnetic stirrer maintaining at 60 °C for 20 min. The solution pH was adjusted to 12 using NaOH (2 M) solution [3]. The resultant precipitate was purified by washing with distilled water three times to remove loosely connected rutin molecules from the ZnO surface and dried at 80 °C for 24 h.

Characterization

The synthesis of ZnO NPs was monitored by UV–visible spectroscopy (JASCO-V-670). UV–Vis spectral analysis was studied in the range from 300 to 800 nm. X-ray diffraction spectroscopic (XRD) analysis was carried out for the determination of the crystalline structure of the ZnO NPs (XPERT-PRO using 40 kV/40 mA current with Cu-Kα radiation). The morphology of the ZnO NPs was studied by field emission electron microscopy (FE-SEM, Sigma-Carl Zeiss). The presences of elements in ZnO NPs were identified and mapped using energy dispersive X-ray spectroscopy (EDX) attached to FE-SEM. Fourier transform infrared spectra of the samples were recorded on FTIR spectrometer from 500 to 4000 cm^{-1} at a resolution of 4 cm^{-1}. The surface charge on ZnO NPs was determined by zeta potential measurement. The zeta potential was measured by analyzing 0.1 g of ZnO NPs in 10 mL of double distilled water using the Zetasizer Nano ZS (Malvern Instruments Ltd., UK). Before zeta potential measurements, samples were sonicated for 5 min and pH was maintained at neutral.

Antibacterial activity determination

In total, four pathogenic bacterial strains, namely *Staphylococcus aureus* (MTCC 3160), *Bacillus subtilis* (MTCC 441), *Klebsiella pneumoniae* (MTCC 530), and *Escherichia coli* (MTCC 443), were obtained from IMTECH and maintained in nutrient agar slants at 4 °C.

The antibacterial activity of the ZnO NPs was tested against the selected bacterial strains through agar disc diffusion method described by Saravanakumar et al. [24]. In brief, each bacterial strain was swabbed (10^5 CFU/mL) on the Meuller-Hinton agar petri plates using sterile cotton swabs. Sterile discs of 5 mm diameter were soaked with different concentrations of ZnO NPs (10, 20 and 40 µg/mL), rutin (20 µg/mL) and control streptomycin sulphate (10 µg/mL). The discs were carefully placed on swabbed plates. After incubation for 24 h at 37 °C, the zone of inhibition was measured.

In vitro antioxidant activity

Antioxidant activity of the synthesized ZnO NPs and rutin was determined by employing the following assays.

DPPH (2,2-diphenyl-1-picrylhydrazyl) assay

DPPH free radical scavenging activity of ZnO NPs and aqueous rutin was determined as described by Abdel-Aziz et al. [25] with few modifications. Briefly, 1.0 mL of 0.1 mM DPPH in methanol was mixed with 1.0 mL each of different concentrations of ZnO NPs (in methanol) and aqueous rutin (ranging from 10 to 50 µg/mL), shaken well and incubated in the dark for 30 min at room temperature. The absorbance was measured at 517 nm using spectrophotometer and DPPH percentage of activity was calculated per the Eq. (1) given in the following.

Hydrogen peroxide (H_2O_2) assay

The H_2O_2 scavenging activity of the ZnO NPs and rutin was determined as described by Anbukkarasi et al. [26] with slight modifications. Briefly, different concentrations of ZnO NPs (in methanol) and aqueous rutin (ranging from 10 to 50 µg/mL) were mixed separately with 50 µL of 5 mM H_2O_2 solution and incubated at room temperature for 20 min. After incubation, the absorbance was measured at 610 nm using spectrophotometer and the percentage of activity was calculated using same equation given

$$\text{Antioxidant activity } (\%) = \left[\left(A_0 - A_1\right)/A_0\right] \times 100 \tag{1}$$

where A_0 was the absorbance of the control and A_1 was the absorbance of the test samples [27].

In vitro cytotoxicity assay

Cytotoxic activity of synthesized ZnO NPs was determined by MTT assay using MCF 7 breast cancer cells as described by Mugade et al. [28] and Nosrati et al. [29] with slight modifications. Briefly, MCF 7 human breast cancer cell line was purchased from National centre for cell science (NCCS), Pune, India. The cells were grown in DMEM supplemented with 10% FBS and streptomycin (1%). 100 µL of MCF 7 cells at a density of 1×10^3 was seeded in a 96-well plate. The seeded cells were incubated for 24 h at 37 °C in a humidified chamber with 5% CO_2. After incubation, different concentrations of ZnO NPs and rutin (25, 50, 75, 100 µg/mL) were added into each well of the plate and incubated for 16 h. After that, the media was replaced with 10 µL of MTT (5 mg/mL of cell culture media) was added to each well and incubated for further 4 h at 37 °C. After incubation, the medium was removed and 100 µL of DMSO was added to each well to dissolve the formazan.

The absorbance was measured using a plate reader (BioRad-680, USA) at 570 nm to determine the cell viability percentage. The percentage of inhibition was calculated using the following formula.

$$\text{Cell vaibility (\%)} = \frac{\text{OD value of experimental sample}}{\text{OD value of experimental control}} \times 100$$

Statistical analysis

All the experimental analysis (antibacterial, antioxidant and cytotoxic activity) was carried out in triplicates and results were expressed as mean ± standard deviation. The statistical data was analyzed by one-way ANOVA using statistical software SPSS (SPSS version 14, IBM Corporation, USA). The significance difference were analysed at $p < 0.05$ or 0.01.

Results and discussion

Synthesis of ZnO NPs

The synthesis of ZnO NPs was carried out using pure bioflavonoid rutin. The synthesis of ZnO NPs was confirmed by the color change from light yellow to white color precipitate [30]. In agreement with our results, *Plectranthus amboinicus* [31], *Ruta graveolens* [17] and *Jacaranda mimosifolia* [32] plant extract-assisted synthesized ZnO NPs formed a white precipitate. The functional groups and molecules present in rutin may be responsible for the reduction of zinc salt to ZnO NPs. This was further confirmed by FTIR studies.

Characterization techniques

UV–Vis spectroscopy

Initially, the synthesis of ZnO NPs was monitored using UV–Vis spectrophotometer. The synthesized ZnO NPs showed highest shift in spectral absorbance peak at 355 nm (Fig. 1). It was reported earlier that the spectral absorbance around 355 nm is a characteristic feature of ZnO NPs [33]. Similar findings have been reported by Lingaraju et al. [17] who documented that the surface plasmon resonance (SPR) absorbance spectrum of ZnO NPs was found at 355 nm.

XRD analysis

XRD analysis can provide information about the crystalline structure of the ZnO NPs. Figure 2 shows the XRD pattern of the synthesized ZnO NPs and the obtained XRD planes [(100), (002), (101), (102), (110), (103), (200), (112), (201), (004) and (002)] were indexed to a hexagonal phase with wurtzite structure

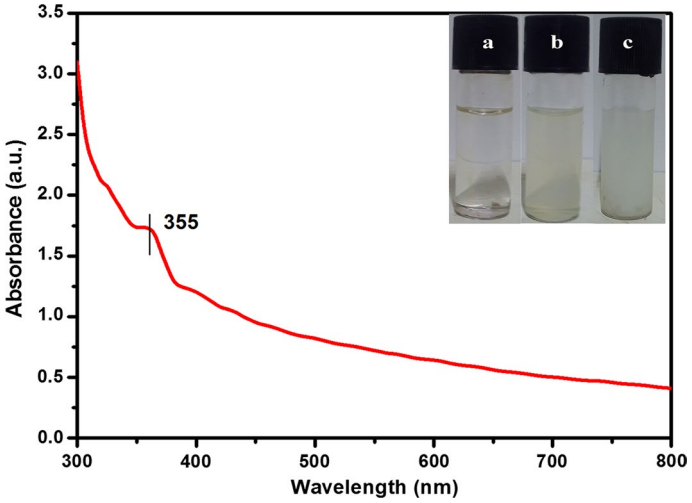

Fig. 1 UV–visible spectra of synthesized ZnO NPs and the inset show the colorization images of (a) zinc sulphate, (b) aqueous rutin, and (c) ZnO NPs

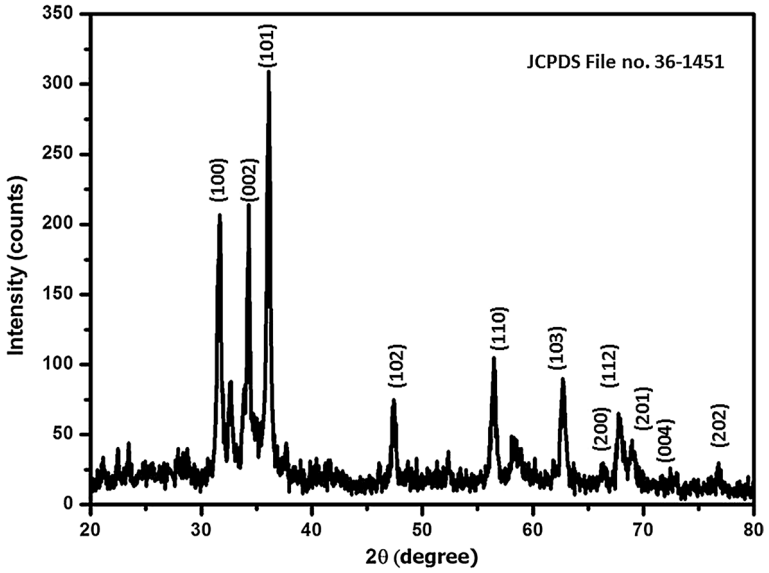

Fig. 2 XRD pattern of ZnO NPs synthesized using bioflavonoid rutin

of ZnO, which also matched with JCPDS card no. 36-1451 [34]. The crystallite size of ZnO NPs was calculated using Debye–Scherrer's formula: $D = 0.9\lambda/\beta \cos \theta$, where "$\lambda$" is the wavelength of X-ray, β is FWHM (full width at half maximum) in radians and θ diffraction angles [35]. The average mean crystallite size

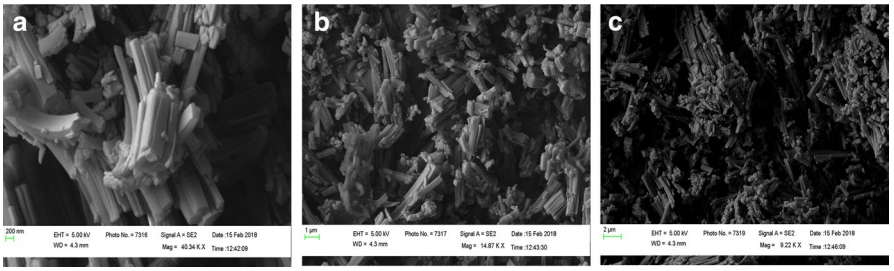

Fig. 3 Electron microscopic (FE-SEM) observation of ZnO NPs at different magnifications

was calculated to be 38 nm. The strong and highest peak obtained at (101) suggested that the polycrystalline structure of synthesized NPs [18].

Electron microscopy and EDX mapping analysis

The morphology of the ZnO NPs was determined by FE-SEM analysis and is shown in Fig. 3. ZnO NPs were found to have rod shape and an average size range of 20–130 nm. Similar to our study, morphology of the biologically synthesized ZnO NPs were exhibited rod shape with varied size range between 80 and 130 nm [36].

EDX spectra and elemental mapping analysis from Fig. 4a represent that there is a signal from Zn together with O, which clearly shows the formation of ZnO NPs. Similar peaks were reported by Vanathi et al. [37]. Figure 4b–e illustrates the corresponding elemental mapping of Zn (Zinc) and O (oxygen) and also it shows the purity of the ZnO NPs by detecting no other elements.

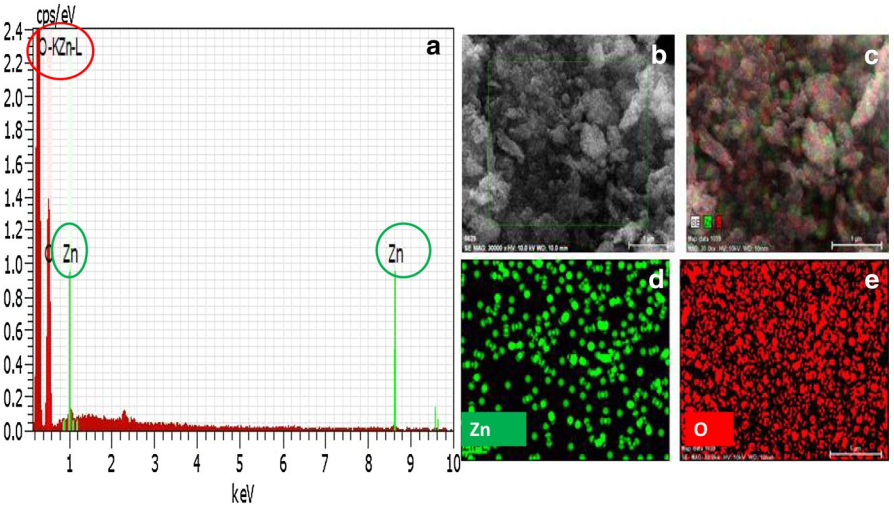

Fig. 4 **a** EDX spectrum of ZnO NPs, and **b–e** their corresponding elemental images

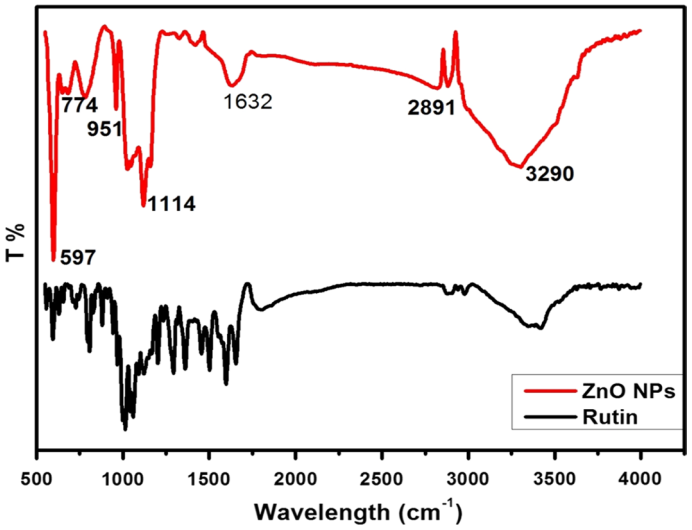

Fig. 5 FTIR spectrum of synthesized ZnO NPs and rutin

FTIR analysis

FTIR spectra of synthesized ZnO NPs and rutin bioflavonoid are shown in Fig. 5. In the ZnO NPs FTIR spectrum, the highest FT-IR peaks at 3290 cm^{-1} are attributed to O–H stretching vibrations of phenols [32, 38]. FTIR spectral bands at 2891, 1632, and 1114 cm^{-1} are assigned to C–H stretching, –C=C–, and C=O stretching of –COOH group [39]. The medium spectral peak at 951 cm^{-1} is assigned to the presence of –OH groups of phenols. The other short peaks from 500 to 800 cm^{-1} were assigned to the presence of metal–oxygen (Zn–O) [32, 40]. This spectroscopic study was confirmed the presence of large amount of phenols. The other FTIR spectrum (Fig. 5) supports the presence of the mentioned compounds that were mainly derived from the rutin bioflavonoid. Rutin ($C_{27}H_{30}O_{16}$) is a poly-phenolic compound containing a large amount of phenolic acids [20]. The presence of these rutin-derived functional groups may be responsible for the reduction, capping, and stabilization of ZnO NPs [27].

Zeta potential measurement

The surface charge on ZnO NPs was determined by Zetasizer. Figure 6 shows the negative charge value (− 24.7 mV) on the synthesized ZnO NPs. The negative potential value from the Zetasizer supports the high stability and dispersity of ZnO NPs [41]. Similar findings were reported by Vimala et al. [42].

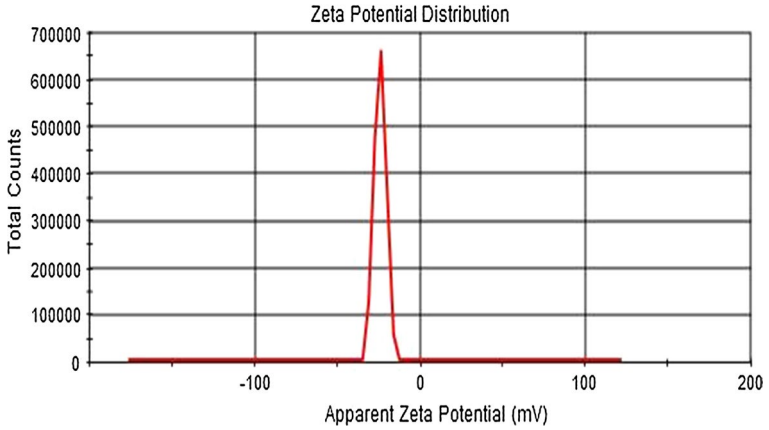

Fig. 6 Zeta potential measurement of synthesized ZnO NPs

Antibacterial activity determination

The synthesized ZnO NPs showed significant activity against common bacterial pathogens. The disk diffusion antibacterial activity of different concentration of ZnO NPs (10, 20 and 40 µg/mL), rutin (20 µg/mL) and control (10 µg/mL) are shown in Fig. 7. The highest antibacterial zone of inhibition was recorded in *E. coli* (24.5 ± 0.30 mm) followed by *K. pneumoniae* (23.5 ± 0.40 mm), *S. aureus* (22 ± 0.30 mm) and *B. subtilis* (20 ± 0.20 mm). The antibacterial zone of inhibition is shown in Table 1. Rutin bioflavonoid does not exhibit any zone of inhibition in the chosen pathogens. Moreover, compared to control streptomycin and rutin, synthesized ZnO NPs showed higher antibacterial activity. Similarly, ZnO NPs synthesized using *Laurus nobilis* leaf extract showed significant antibacterial activity against *P. aeruginosa* and *S. aureus* [43]. The results of antibacterial properties of ZnO NPs differ based on the cell wall nature of Gram-negative and Gram-positive bacteria [44, 45]. In the present study, synthesized ZnO NPs showed higher bactericidal activity against Gram-negative bacteria (*E. coli* and *K. pneumoniae*) compared to Gram-positive bacterial pathogens (*S. aureus* and *B. subtilis*). Similar findings were reported by Bhuyan et al. [46]. This is due to the permeable capability of ZnO NPs into the cell wall of Gram-positive and Gram-negative bacteria [47].

In vitro antioxidant activities

The scavenging ability of ZnO NPs was determined using DPPH and H_2O_2 assays. In the DPPH assay, it was observed that the free radical scavenging ability of ZnO NPs and rutin increased in a concentration-dependent manner. The percentage of DPPH activity increased with increasing concentration of the samples (Fig. 8a). Similar to our report, ZnO NPs synthesized using stem barks extract of *R. graveolens* exhibited concentration depended manner of DPPH antioxidant activity [3]. In the present study, the antioxidant capability of synthesized ZnO NPs showed

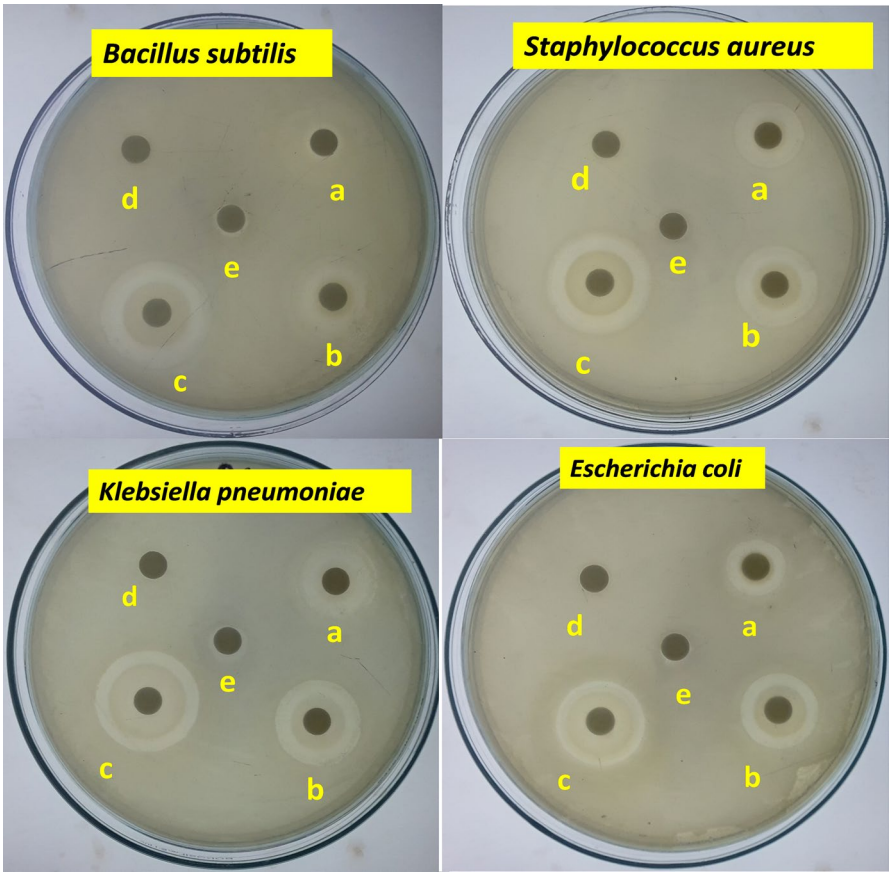

Fig. 7 Antibacterial activity of ZnO NPs against Gram-positive and Gram-negative bacterial pathogens: (a–c) different concentration of ZnO NPs (10, 20 and 40 µg/mL), (d) rutin (20 µg/mL) and (e) control streptomycin (10 µg/mL)

Table 1 Antibacterial activity: zone of inhibition (ZOI) against Gram-positive and Gram-negative bacterial pathogens

S. no.	Bacterial pathogens	ZnO NPs			Control[a]	Rutin
		10 µg/mL	20 µg/mL	40 µg/mL	10 µg/mL	20 µg/mL
1	*B. subtilis* (MTCC 441)	7 ± 0.30	13.5 ± 0.20	20 ± 0.20	7 ± 0.50	–
2	*S. aureus* (MTCC 3160)	11 ± 0.70	17 ± 0.40	22 ± 0.30	7.3 ± 0.20	–
3	*K. pneumoniae* (MTCC 530)	11.5 ± 0.20	18.5 ± 0.20	23.5 ± 0.40	8.2 ± 0.20	–
4	*E. coli* (MTCC 443)	12 ± 0.25	19 ± 0.50	24.5 ± 0.30	7.2 ± 0.50	–

Values represent the mean (±) standard error of three independent antibacterial assays. Zone of inhibition measured as millimetre (mm) in diameter

[a]Streptomycin sulphate (10 µg/mL) used as a control

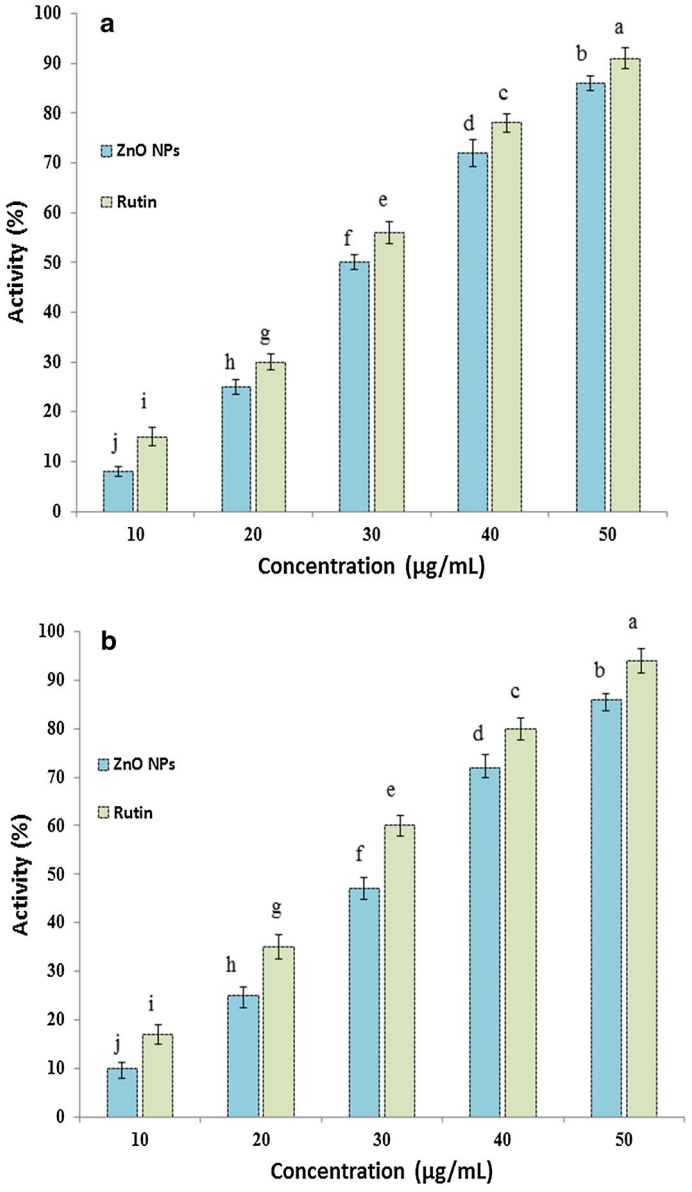

Fig. 8 Antioxidant activity of ZnO NPs and rutin bioflavonoid, **a** DPPH and **b** H_2O_2 assay. Values represent the mean (±) standard error of three independent antioxidant assays

potentially similar activity to rutin. The free radical scavenging ability of ZnO NPs might be due to the presence of phenols that have the ability to donate the H in their OH groups [48, 49].

The H_2O_2 antioxidant assay was performed to evaluate the free radical scavenging ability of the synthesized ZnO NPs. The H_2O_2 inhibition percentage of ZnO

NPs increased with increasing concentration of ZnO NPs (Fig. 8b). The H_2O_2 assay mainly depends on the presence of phenolic compounds in the ZnO NPs [26, 49]. Similar findings were documented by Rehana et al. [50] who reported that the significant H_2O_2 scavenging activity of ZnO NPs synthesized using plant extract.

In vitro cytotoxicity assay

Cytotoxic properties of synthesized ZnO NPs and rutin compounds were evaluated against MCF-7 breast cancer cells by MTT assay. Synthesized ZnO NPs and rutin bioflavonoid showed concentration dependent cytotoxic activity against breast cancer cells. The results showed a significant decrease in the viability of MCF-7 breast cancer cells when the concentration of ZnO NPs was increased from 10 to 50 µg/mL (Fig. 9). Similar findings were reported by Malaikozhundan et al. [51], who observed that dose-depended cytotoxic activity of ZnO NPs against MCF-7 breast cancer cells. The synthesized ZnO NPs, bioflavonoid rutin, and control (doxorubicin) induced 50% (IC_{50}) of inhibition activity against MCF-7 cells at the concentration of 27.05 ± 0.50, 35 ± 0.50 and 18.03 ± 0.30 µg/mL, respectively. Pure rutin bioflavonoid showed potential inhibiting activity against tested cell line. However, synthesized ZnO NPs showed higher activity compared to rutin bio-compound. Similar findings were documented by Sisubalan et al. [19] who reported that the ZnO NPs synthesized using leaf extract of *Rubia cordifolia* showed significant inhibiting activity against osteosarcoma cell lines. It was reported that the cytotoxic activity of metal oxide nanoparticles were dependent on the shape, size and capping agents of the nanoparticles [19, 52, 53].

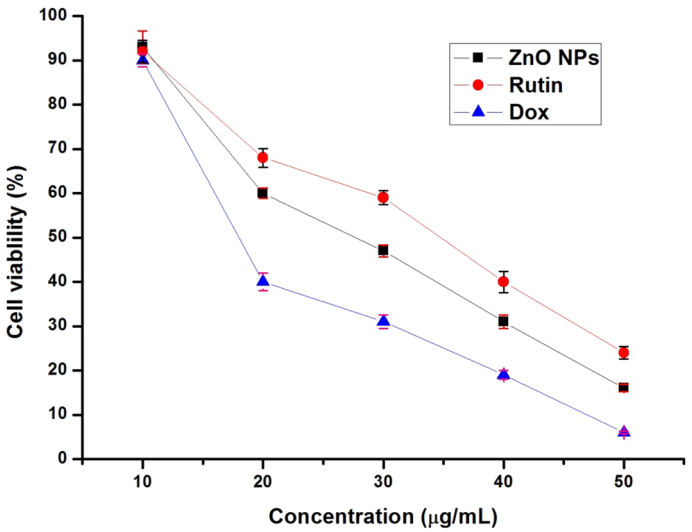

Fig. 9 MCF-7 breast cancer cell viability results against various concentrations of ZnO NPs, rutin and control. Values represent the mean (±) standard error of three independent assays

Conclusion

The present study was an eco-friendly synthesis of ZnO NPs using pure bioflavonoid rutin. Our synthesis protocol follows a facile green chemistry method. To our knowledge, this is the first report on synthesis of ZnO NPs using pure single bioflavonoid rutin compound. Synthesized nanoparticles have exhibited rod shape with varied size of 20–130 nm. The bioflavonoid rutin assisted synthesized ZnO NPs displayed significant antibacterial activity against both Gram-positive and Gram-negative bacteria. The synthesized NPs have exhibited potential free radical scavenging ability, which was confirmed by DPPH and H_2O_2 assay. In addition, ZnO NPs was effectively inhibiting the growth of MCF-7 cancer cells under in vitro condition. Thus, we believe that the synthesized ZnO NPs in this study might be used as nano-bioflavonoids in biomedical and pharmaceutical industries.

Acknowledgements The authors like to thank Department of Science and Technology (DST-FIST) (Grant No. DST-FIST/120/2012), India for providing the fund for establishing laboratory facilities to the Department of Biotechnology, Kongunadu Arts and Science College and we acknowledge the South Indian Textile Research Association and Research (SITRA), and Department of Nanoscience and Nanotechnology, Bharathiar University, Coimbatore for extending their material characterization facilities.

Compliance with ethical standards

Conflict of interest The authors declare that they have no conflict of interest.

References

1. S. Sabir, M. Arshad, S.K. Chaudhari, Sci. World J. **2014**, 1 (2014)
2. S.P. Rajendran, K. Sengodan, J. Nanosci. **2017**, 1 (2017)
3. P. Jamdagni, P. Khatri, J.S. Rana, J. King Saud Univ. Sci. **30**, 168 (2016)
4. A.A. Jahagirdar, N. Dhananjaya, D.L. Monika, C.R. Kesavulu, H. Nagabhushana, S.C. Sharma, B.M. Nagabhushana, C. Shivakumara, J.L. Rao, R.P.S. Chakradhar, Spectrochim. Acta A Mol. Biomol. Spectrosc. **104**, 512 (2013)
5. R.K. Sharma, R. Ghose, Ceram. Int. **41**, 967 (2015)
6. M. Ristić, S. Musić, M. Ivanda, S. Popović, J. Alloys Compd. **397**, L1 (2005)
7. M. Hasanpoor, M. Aliofkhazraei, H. Delavari, Procedia Mater. Sci. **11**, 320 (2015)
8. A.E. Kandjani, M.F. Tabriz, B. Pourabbas, Mater. Res. Bull. **43**, 645 (2008)
9. S. Baskoutas, P. Giabouranis, S.N. Yannopoulos, V. Dracopoulos, L. Toth, A. Chrissanthopoulos, N. Bouropoulos, Thin Solid Films **515**, 8461 (2007)
10. H. Wei, Y. Wu, N. Lun, C. Hu, Mater. Sci. Eng. A **393**, 80 (2005)
11. S.M. Pourmortazavi, Z. Marashianpour, M.S. Karimi, M. Mohammad-Zadeh, J. Mol. Struct. **1099**, 232 (2015)
12. T. Karnan, S.A.S. Selvakumar, J. Mol. Struct. **1125**, 358 (2016)
13. O.J. Nava, C.A. Soto-Robles, C.M. Gómez-Gutiérrez, A.R. Vilchis-Nestor, A. Castro-Beltrán, A. Olivas, P.A. Luque, J. Mol. Struct. **1147**, 1 (2017)
14. R. Dobrucka, J. Długaszewska, Saudi J. Biol. Sci. **23**, 517 (2016)
15. D. Davies, D. Davies, Microbiol. Mol. Biol. Rev. **74**, 417 (2010)
16. R. Krishnamoorthy, J. Athinarayanan, V.S. Periasamy, A.R. Adisa, M.A. Al-Shuniaber, M.A. Gassem, A.A. Alshatwi, Microb. Pathog. **120**, 85 (2018)
17. K. Lingaraju, H.R. Naika, K. Manjunath, R.B. Basavaraj, H. Nagabhushana, G. Nagaraju, D. Suresh, Appl. Nanosci. **6**, 703 (2016)
18. J. Ali, R. Irshad, B. Li, K. Tahir, A. Ahmad, M. Shakeel, N.U. Khan, Z.U.H. Khan, J. Photochem. Photobiol. B **183**, 349 (2018)
19. N. Sisubalan, V.S. Ramkumar, A. Pugazhendhi, C. Karthikeyan, K. Indira, K. Gopinath, A.S.H. Hameed, M.H.G. Basha, Environ. Sci. Pollut. Res. Int. **25**, 10482 (2017)

20. M.I. Azevedo, A.F. Pereira, R.B. Nogueira, F.B. Rolim, G.A. Brito, D.V.T. Wong, R.C. Lima-Júnior, R. de Albuquerque Ribeiro, M.L. Vale, M. Pain. **9**, 53 (2013)
21. G. Di Carlo, N. Mascolo, A.A. Izzo, F. Capasso, Life Sci. **65**, 337 (1999)
22. S. Kreft, M. Knapp, I. Kreft, J. Agric. Food Chem. **47**, 4649 (1999)
23. F. Wu, J. Chen, L.M. Fan, K. Liu, N. Zhang, S.W. Li, H. Zhu, H.C. Gao, Exp. Ther. Med. **14**, 27 (2017)
24. K. Saravanakumar, R. Chelliah, S.R. Ramakrishnan, K. Kathiresan, D.H. Oh, M.H. Wang, Microb. Pathog. **115**, 338 (2018)
25. M.S. Abdel-Aziz, M.S. Shaheen, A.A. El-Nekeety, M.A. Abdel-Wahhab, J. Saudi Chem. Soc. **18**, 356 (2014)
26. M. Anbukkarasi, P.A. Thomas, J.R. Sheu, P. Geraldine, Biomed. Pharmacother. **91**, 467 (2017)
27. D. Bharathi, M.D. Josebin, S. Vasantharaj, V. Bhuvaneshwari, J. Nanostruct. Chem. **8**, 83 (2018)
28. M. Mugade, M. Patole, V. Pokharkar, Biomed. Pharmacother. **91**, 95 (2017)
29. H. Nosrati, M. Adibtabar, A. Sharafi, H. Danafar, M. HamidrezaKheiri, Drug Dev. Ind. Pharm. **44**, 1377 (2018)
30. B. Malaikozhundan, B. Vaseeharan, S. Vijayakumar, M.P. Thangaraj, J. Photochem. Photobiol. B **174**, 306 (2017)
31. S. Vijayakumar, G. Vinoj, B. Malaikozhundan, S. Shanthi, B. Vaseeharan, Spectrochim. Acta A Mol. Biomol. Spectrosc. **137**, 886 (2015)
32. D. Sharma, M.I. Sabela, S. Kanchi, P.S. Mdluli, G. Singh, T.A. Stenström, K. Bisetty, J. Photochem. Photobiol. B **162**, 199 (2016)
33. S.K. Chaudhuri, L. Malodia, Appl. Nanosci. **7**, 501 (2017)
34. S.A. Ansari, S.G. Ansari, H. Foaud, M.H. Cho, New J. Chem. **41**, 9314 (2017)
35. M. Salehiabar, H. Nosrati, S. Davaran, H. Danafar, H.K. Manjili, Drug Res. **68**, 280 (2018)
36. J. Sujatha, S. Asokan, S. Rajeshkumar, J. Microbiol. Biotechnol. Food Sci. **7**, 348 (2018)
37. P. Vanathi, P. Rajiv, S. Narendhran, S. Rajeshwari, P.K. Rahman, R. Venckatesh, Mater. Lett. **134**, 13 (2014)
38. K. Steffy, N. Shanthi, A.S. Maroky, S. Selvakumar, J. Adv. Res. **9**, 69 (2018)
39. R. Mukhopadhyay, J. Kazi, M.C. Debnath, Biomed. Pharmacother. **97**, 1373 (2018)
40. D. Vaidehi, V. Bhuvaneshwari, D. Bharathi, B.P. Sheetal, Mater. Res. Express **5**, 085403 (2018)
41. R. Marsalek, APCBEE Procedia **9**, 13 (2014)
42. K. Vimala, S. Sundarraj, M. Paulpandi, S. Vengatesan, S. Kannan, Process Biochem. **49**, 160 (2014)
43. S. Vijayakumar, B. Vaseeharan, B. Malaikozhundan, M. Shobiya, Biomed. Pharmacother. **84**, 1213 (2016)
44. S. Sathiyavimal, S. Vasantharaj, D. Bharathi, S. Mythili, E. Manikandan, S.S. Kumar, A. Pugazhendhi, J. Photochem. Photobiol. B **188**, 126 (2018)
45. D. Bharathi, S. Vasantharaj, V. Bhuvaneshwari, Mater. Res. Express **5**, 055404 (2018)
46. T. Bhuyan, K. Mishra, M. Khanuja, R. Prasad, A. Varma, Mater. Sci. Semicond. Proc. **32**, 55 (2015)
47. A.M. Fayaz, K. Balaji, M. Girilal, R. Yadav, P.T. Kalaichelvan, R. Venketesan, Nanomed. Nanotechnol. **6**, 103 (2010)
48. K. Prabu, A. Rajasekaran, D. Bharathi, S. Ramalakshmi, J. King Saud Univ. Sci. (2018). https://doi.org/10.1016/j.jksus.2018.04.025
49. D. Bharathi, V. Bhuvaneshwari, BioNanoScience. (2018). https://doi.org/10.1007/s12668-018-0577-5
50. D. Rehana, D. Mahendiran, R.S. Kumar, A.K. Rahiman, Bioprocess Biosyst. Eng. **40**, 943 (2017)
51. B. Malaikozhundan, B. Vaseeharan, S. Vijayakumar, K. Pandiselvi, M.A.R. Kalanjiam, K. Murugan, G. Benelli, Microb. Pathog. **104**, 268 (2017)
52. A. Boroumand Moghaddam, M. Moniri, S. Azizi, R. Abdul Rahim, A. Bin Ariff, M. Navaderi, R. Mohamad, Genes **8**, 281 (2017)
53. H. Nosrati, A. Mojtahedi, H. Danafar, H. KheiriManjili, J. Biomed. Mater. Res. A **106**, 1646 (2018)